PHYSOR 2004 -The Physics of Fuel Cycles and Advanced Nuclear Systems: Global Developments
Chicago, Illinois, April 25-29, 2004, on CD-ROM, American Nuclear Society, Lagrange Park, IL. (2004)

Thermal Neutron Time-of-Flight Spectroscopy at Penn State using a Single-Disk Chopper

J. Niederhaus, J. Brenizer*, K. Ünlü
Department of Mechanical and Nuclear Engineering
The Pennsylvania State University
138 Reber Building
University Park, PA 16802

A single-disk, "slow" chopper system has been developed at the Penn State University Radiation Science and Engineering Center (RSEC) for the purpose of energy spectrum measurements on thermal neutron beams ($E < 1$ eV). The primary beam at PSU RSEC was gated with a single-disk neutron chopper, and the distribution in neutron time-of-flight (TOF) across a known distance was recorded. A procedure was defined whereby the recorded TOF distribution was corrected for various experimental conditions and transformed to yield the velocity and energy spectrum of neutrons in the beam. These data were compared to distributions derived from models based on the Maxwell-Boltzmann distribution. This comparison facilitated characterization of the beam and evaluation of the instrument's usefulness and accuracy in spectroscopic measurements.

KEYWORDS: neutron spectroscopy, time of flight, thermal neutron

1. Introduction

Accurate measurement of neutron spectra often becomes necessary when neutron beams are used in experimental applications. Such spectra can be obtained simply and conveniently using time-of-flight (TOF) spectroscopy. In this method, the energies of neutrons within a thermal beam are obtained from their flight times across a known distance. No measurement of the energy deposited by neutrons in the detector or imparted to secondary particles is necessary. However, neutrons whose flight times are to be measured must all enter the flight path at or near the same point in time.

For a continuous neutron source such as a typical research reactor, a device is needed to pass neutrons to a detector with a specified time period. A single disk chopper functions adequately in this capacity for neutrons whose energies are less than about 1 eV. A neutron-opaque disk rotates on an axis parallel to the neutron beam. A short, narrow slit cut along the disk radius passes through the beam once per rotation, transmitting a momentary burst of neutrons. If this burst is short enough relative to the flight times of neutrons to an adjacent detector, then it is possible to resolve the difference in flight times of neutrons at various energies. In that case, counts recorded in successive time bins by the detector can be manipulated to yield a distribution of transmitted beam intensity with respect to time-of-flight. This TOF spectrum can then be

* Corresponding author, Tel. 814-863-6394, FAX 814-865-1280, E-mail: brenizer@engr.psu.edu

converted to velocity and energy spectra by relating the time-of-flight to the neutron speed and energy. This simple method provides a convenient and effective means of measuring the spectrum in thermal neutron beams such as those typically used at many research reactor facilities.

2. Penn State RSEC reactor and neutron beam equipment

A disk chopper of this type was used to obtain velocity and energy spectra for the primary neutron beam at the Penn State University Radiation Science and Engineering Center (RSEC). The 1 MWt TRIGA Mark III "swimming pool" reactor at RSEC was used to generate neutrons in this beam. At RSEC, an air-filled beam tube carries thermalized neutrons from the pool-temperature moderator tank through the reactor pool and pool wall to a beam port located in the RSEC neutron beam laboratory. This tube has a direct view of the 82-liter D_2O tank, but is oriented tangentially with respect to the core. The beam tube consists of four joined segments of aluminum pipe, with inner diameters varying from 15.2 cm nearest the D_2O tank to 19.1 cm at the beam port, and a total length of 340 cm. The only material that obstructs the line of sight within the beam is aluminum pipe wall at the joints between sections of tube, and a solid 5-cm thick bismuth filter disk located at the coupling between the beam tube and moderator tank. Two collimator pieces were placed at the end of the beam tube in order to obtain a 1.9 cm diameter neutron beam. The chopper and detection system used in this experiment were placed in the RSEC neutron beam laboratory, adjacent to the primary beam port. This setup allowed for a maximum spectroscopy flight path length of about 3 m. [1-2]. A schematic of the RSEC reactor core, moderator assembly, beam tube, and neutron chopper TOF system is given in Figure 1.

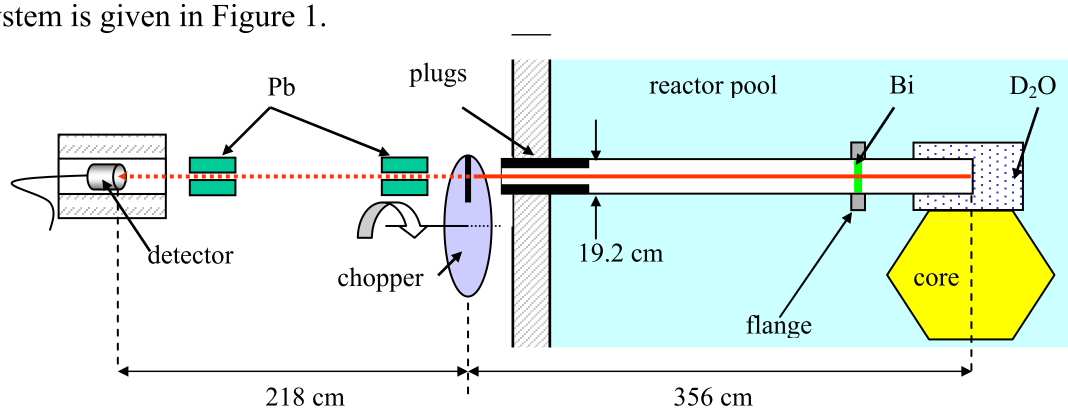

Fig.1. Schematic layout of Breazeale Nuclear Reactor core, beam port #4, and neutron chopper time-of-flight system.

3. Experimental setup and technique for neutron TOF spectroscopy

3.1 Neutron chopper device

The single-disk neutron chopper apparatus was acquired from Cornell University [3-4]. The chopper itself consists of a 1.6-mm thick aluminum disk, 305 mm in diameter, coated on both faces with gadolinium paint (Gd_2O_3/epoxy mixture) to absorb thermal neutrons. This is overlaid with 1.02-mm thick cadmium sheet on both faces. The disk is equipped with a single narrow radial slit. The slit has a trapezoidal shape to reduce partial-opening effects, and extends 5 cm along the disk radius, with a width of 0.7 mm near the axis, and 1 mm near the disk edge. The inner edge of the slit is located 95 mm from the disk axis.

The disk is housed between two aluminum faceplates and turns at a constant rotational period of 115 ms (522 rpm). It transmits a 384-μs burst of neutrons once per rotation, as the slit passes a pair of apertures formed by 1-mm wide slits in a pair of cadmium plates that are bolted to the upstream and downstream faceplates and centered in the beam. The chopper disk was positioned 356 cm downstream from the head of the beam tube inside the D_2O tank, 218 cm upstream from the detection system. A schematic drawing of single-disk chopper used in this study is given in Figure 2.

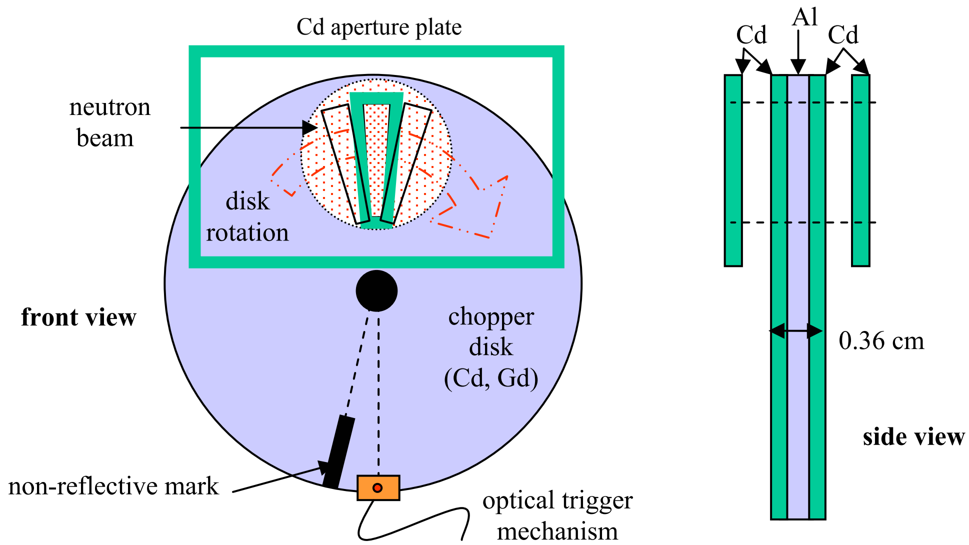

Fig. 2. Schematic of single-disk neutron chopper

3.2 Collimation

A total of four collimators were added to the beam to facilitate use of the chopper: two in the beam port, and two along the spectroscopy flight path. To reduce the size, divergence, and gamma component of the beam, two 35.6-cm long annular collimator plugs made of lead and concrete were fitted to the beam tube and inserted end-to-end in the tube at the beam port. The upstream collimator annulus had an inner diameter of 3.8 cm, and the downstream annulus had an inner diameter of 1.9 cm. Thus, with the beam port collimators in place, the chopper slit was illuminated by a 1.9-cm collimated beam.

Two more collimators were added along the neutron flight path. Each flight path collimator consisted of a narrowly-spaced pair of 10.2-cm deep lead blocks placed on either side of the beam. One pair was positioned at the upstream end of the flight path, immediately adjacent to the cadmium aperture on the chopper housing, and the other pair at the downstream end of the flight path, adjacent to the detector. The gap between the upstream blocks was 1 mm, centered on the aperture slit. The gap between the downstream blocks was 12.7 mm, centered on the detector face. The flight path collimators further reduced the time-independent gamma component of the beam incident on the detector.

3.3 Data acquisition system

Neutron events were observed via (n,α) interactions in a LiI(Eu) scintillator crystal that was coupled to a Photo Multiplier Tube (PMT). PMT pulses were counted in sequential time channels in a multi-channel scaler (MCS) system. Pulse-height discrimination at the PMT output allowed only a minimal number of gamma events to be included in the input signal analyzed by the MCS system.

The MCS system recorded counts in 1024 channels, with a dwell time of 20 μs. A single pass or "sweep" over the complete set of channels was performed once per chopper rotation, synchronized to the slit opening by a photodiode trigger. A TOF spectrum was acquired over 150,000 passes at a reactor power of 1 MWt. A total of approximately 70,000 counts per channel were accumulated at the peak of the neutron pulse, including a constant background level of approximately 17,000 counts per channel.

4. Determinate corrections to observed data

The raw data recorded in the MCS system had the form of a set of data points (i,N_i), where i is the channel index (i = 0,1023) and N_i is the raw total number of counts accumulated in channel i during the experimental run. Each data channel was assigned a mean flight time t_i, velocity v_i, and energy E_i, using the dwell time per channel (20 μs), synchronization time (79 μs), flight distance (218 cm), and neutron mass.

A procedure was established whereby the number of recorded counts in each channel N_i was used to find the unattenuated neutron flux $\Delta\phi_i$, which is the flux only of neutrons that arrived in data channel i, and were thus assumed to have energy E_i and velocity v_i. This procedure accounted for background radiation, dead time effects in the detection system, detector efficiency, and attenuation of the beam by moist air in the flight path.

4.1 Dead time effects and background radiation

Due to the high count rates, dead time effects were substantial in the peak flux region of the recorded data. For simplicity in this experiment, the system was assumed to be nonparalyzable, *i.e.*, the total system dead time τ was a constant at all count rates. The measured system dead time was 13.4 μs.

The nominal background level B was then determined by averaging the number of counts recorded in the time-independent region of the raw data. Assuming a nonparalyzable system, the true number of background-corrected counts that would have been observed in MCS channel i was then calculated from N_i and B as

$$N_i' = N_i\left(1-\frac{\tau N_i}{t_c}\right)^{-1} - B\left(1-\frac{\tau B}{t_c}\right)^{-1}, \quad (1)$$

where t_c is the total counting time per channel, given as the product of the dwell time per channel and the total number of MCS passes. Dividing again by the total counting time per channel yielded the true neutron count rate R_i in channel i.

4.2 Detection efficiency

The neutron flux incident at the detector surface was determined from R_i, using the detection efficiency of the scintillator crystal. Assuming that the dominant mode of attenuation in the scintillator crystal was the (n,α) reaction, the neutron flux $\Delta\phi_0$ incident on the surface of the scintillator for MCS channel i was calculated as

$$\Delta\phi_{0,i} = \frac{R_i}{A\left[1-\exp\left(-\Sigma_{Li,i}T\right)\right]}, \tag{2}$$

where A is the exposed area of the crystal (cm^2), T is its thickness (cm), and $\Sigma_{Li,i}$ is the $^6Li(n,\alpha)^3H$ cross section (cm^{-1}) for the crystal material, evaluated at energy E_i.

4.3 Attenuation in air

An additional factor was applied to the experimental data in each channel to account for scattering in the 218-cm column of moist air between the chopper and the detector. Macroscopic scattering cross sections $\Sigma_{air,i}$ were calculated assuming 70% relative humidity and standard air composition, evaluated at energies E_i. Assuming that a single scattering interaction removed a neutron from the beam, the neutron flux $\Delta\phi_i$ at the entrance to the flight path was determined as

$$\Delta\phi_i = \Delta\phi_{0,i}\exp\left(\Sigma_{air,i}\cdot 218\,\text{cm}\right). \tag{3}$$

The neutron flux per unit time-of-flight for channel i was found by dividing this flux by the dwell time per channel, Δt. In this way, each (i,N_i) data point was transformed to yield the TOF distribution data point $(t_i, \Delta\phi_i/\Delta t)$.

5. Spectrum transformation for observed data

Since the dwell time per channel was very small (Δt = 20 μs), the following approximation holds:

$$\frac{\Delta\phi_i}{\Delta t} \cong \left(\frac{d\phi}{dt}\right)_i \tag{4}$$

That is, the flux per unit time-of-flight for channel i can be regarded as the first derivative of the flux with respect to time-of-flight, evaluated at time t_i. This constitutes a TOF spectrum. The velocity spectrum $(d\phi/dv)_i$ and energy spectrum $(d\phi/dE)_i$ data were obtained from the TOF spectrum data $(d\phi/dt)_i$ by applying the chain rule: [5]

$$\left(\frac{d\phi}{dv}\right)_i = \left|\left(\frac{d\phi}{dt}\right)_i \frac{dt}{dv_i}\right| = \left(\frac{d\phi}{dt}\right)_i \frac{t_i^2}{D} \quad (5)$$

$$\left(\frac{d\phi}{dE}\right)_i = \left|\left(\frac{d\phi}{dv}\right)_i \frac{dv_i}{dE_i}\right| = \left(\frac{d\phi}{dv}\right)_i \frac{1.6\times10^{-19}}{mv_i} \quad (6)$$

The $(d\phi/dv)_i$ term represents the differential flux per unit neutron speed, and was given in units of $cm^{-2}s^{-1}$ per m/s. The $(d\phi/dt)_i$ term represents the differential flux per unit neutron energy, and was given in units of $cm^{-2}s^{-1}$ per eV. This method conserves the flux recorded in each channel. Equations 4 through 6 can be rearranged to yield

$$\left|\left(\frac{d\phi}{dt}\right)_i \Delta t\right| = \left|\left(\frac{d\phi}{dv}\right)_i dv_i\right| = \left|\left(\frac{d\phi}{dE}\right)_i dE_i\right| \cong \Delta\phi_i\,. \quad (7)$$

The velocity spectrum was constructed by plotting $(d\phi/dv)_i$ against the velocity ordinates v_i, and the energy spectrum was constructed by plotting $(d\phi/dE)_i$ against the energy ordinates E_i. These spectra are shown in Figures 3 and 4.

6. Experimental error analysis

The measurement error in this experiment was dominated by two components: the error in the flight time, σ_t, and the error in the number of counts per channel, σ_N. Due to the width of the chopper slit, error was introduced into the measured flight time, since neutrons could enter the flight path while the slit/aperture system was only partially open. The illuminated area of the slit-aperture system behaved like a Gaussian function in time, with a half-width of 192 μs. Therefore, it was estimated that 68% of all neutrons transmitted by the chopper entered the flight path within ±74.4 μs of the moment of full alignment. This represents the standard deviation σ_t in the recorded time of flight.

Assuming that neutron counts followed a standard normal distribution, the standard deviation $\sigma_{N,i}$ in the raw number of counts recorded per channel was $(N_i)^{1/2}$. The total error σ_t in the spectrum data (vertical error bar) was calculated for each channel using the error propagation formula:

$$\sigma_i^2 = \left(\frac{\partial S}{\partial t}\right)_i^2 \sigma_t^2 + \left(\frac{\partial S}{\partial N}\right)_i^2 \sigma_{N,i}^2\,, \quad (8)$$

where S represents the spectrum data $(d\phi/dv)_i$ or $(d\phi/dE)_i$. Similarly, horizontal error bars were added at each data point, which represent the error associated with the values of v_i and E_i due to the error of σ_t in the measured flight time.

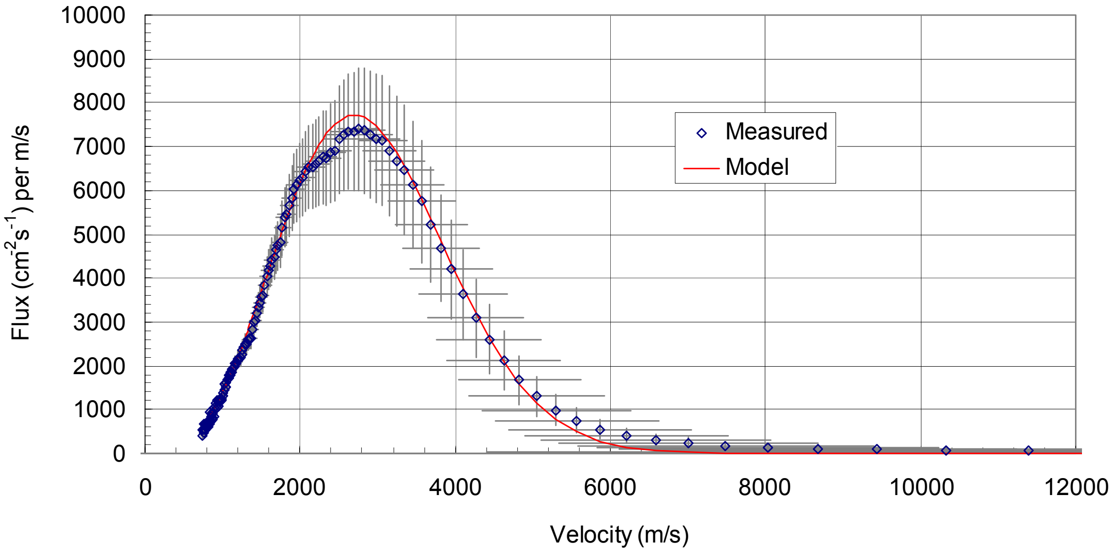

Fig. 3. Neutron velocity spectrum, with ±1σ horizontal and vertical error bars.

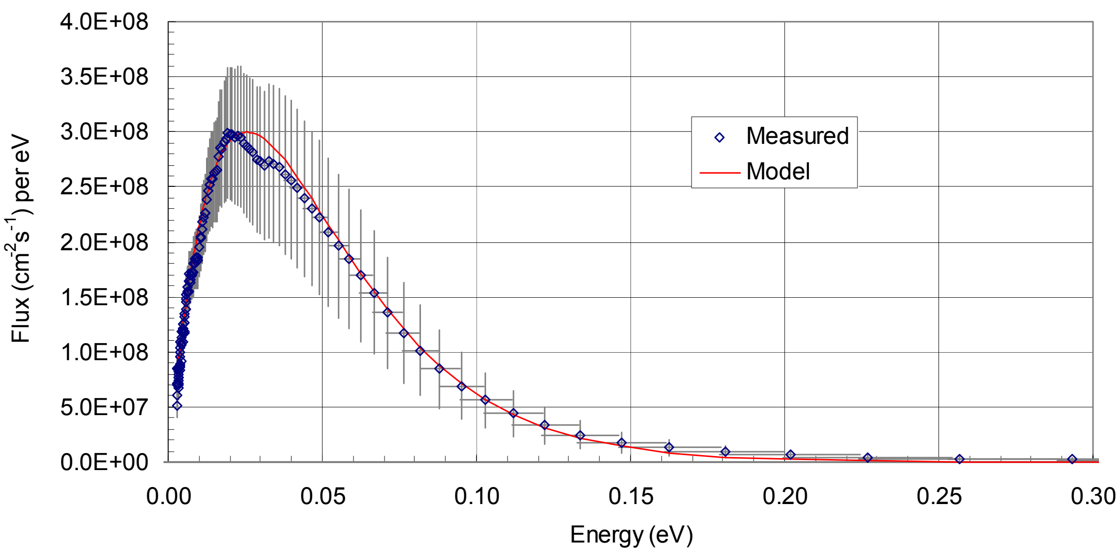

Fig. 4. Neutron energy spectrum, with ±1σ horizontal and vertical error bars.

The error levels indicated by the results shown in Figures 3 and 4 are very high, up to 30% and more, especially at higher neutron energies. However, the acquisition of a smooth spectrum was possible because the TOF error was symmetric about the mean flight time, due to the symmetric shape of the chopper slit. The error in the spectrum data could be dramatically reduced by using a smaller chopper slit and faster rotation speed. However, the number of sweeps would have to be increased to maintain or increase N_i. Better accuracy might also be obtained by lengthening the neutron flight path.

7. Thermal spectrum model based on the Maxwell-Boltzmann distribution

The measured spectra in the RSEC primary beam were expected to correspond closely to a pure thermal spectrum, as dictated by the bulk temperature T in the D_2O tank (20°C). In that case, the differential number density dn of neutrons in the moderator region with velocity v in dv could be described by the Maxwell-Boltzmann formula. The differential element of flux corresponding to this speed and number density of neutrons would then be $d\phi = v \cdot dn$. Hence, the differential neutron flux per unit velocity emerging from the moderator region is described by the Maxwell-Boltzmann formula, modified by a factor of v and appropriately renormalized:

$$\frac{d\phi}{dv}(v) = \frac{\phi_m}{2}\left(\frac{m}{kT}\right)^2 v^3 \exp\left(-\frac{mv^2}{2kT}\right), \tag{9}$$

where ϕ_m is the total neutron flux emerging from the moderator region, and k is Boltzmann's constant. Similarly, the Maxwell-Boltzmann distribution in energy is modified by a factor of $E^{1/2}$ to describe the differential flux per unit energy:

$$\frac{d\phi}{dE}(E) = \phi_m \left(\frac{1}{kT}\right)^2 E \exp\left(-\frac{E}{kT}\right) \tag{10}$$

These formulae represent the neutron flux distributions in velocity and energy that would have been observed at the edge of the moderator region. In traveling from the moderator to the chopper position, the neutron flux was reduced by an energy-dependent attenuation factor f_{air}. The total path length of air traversed by neutrons between the D_2O tank and the chopper was D_0 = 351 cm. Thus, the attenuation factor was calculated as

$$f_{air}(E_i) = f_{air,i} = \exp(-\Sigma_{air,i} D_0) \tag{11}$$

Hence, the expected neutron velocity and energy distributions at the chopper location were calculated as

$$\frac{d\phi}{dv}(v_i) = f_{air,i}\frac{\phi_m}{2}\left(\frac{m}{kT}\right)^2 v_i^3 \exp\left(-\frac{mv_i^2}{2kT}\right) \tag{12}$$

$$\frac{d\phi}{dE}(E_i) = f_{air,i}\phi_m \left(\frac{1}{kT}\right)^2 E_i \exp\left(-\frac{E_i}{kT}\right) \tag{13}$$

The total neutron flux ϕ_m emerging from the moderator was found from $\Delta\phi_i$ and f_{air}:

$$\phi_m = \sum_i \frac{\Delta\phi_i}{f_{air,i}} \tag{14}$$

This yielded a Maxwellian-based model, appropriately normalized for comparison to measured velocity and energy spectra, as shown in Figures 3 and 4.

8. Analysis of experimentally-measured spectra

The measured spectra in Figures 3 and 4 show a definitive thermal shape, which closely matches the modeled spectra. This indicates that the chopper spectrometer has properly captured the expected thermal spectrum. However, the experimental spectra deviate from the modeled spectra at speeds near 2400 m/s and energies near 0.03 eV. This deviation affects the location of the peak in the data, so that the most probable neutron speed in the beam is 2623 m/s, and the most probable energy is 0.0194 eV. From Equations 12 and 13, the expected values are 2687 m/s and 0.0253 eV, respectively. This deviation is most likely the result of energy-selective crystalline scattering effects that occur in the 5-cm thick bismuth filter inserted in the RSEC beam tube [6].

The chopper spectrometer was used to measure the spectrum at lower reactor power levels, in order to determine whether its shape changes with the reactor power. Raw data was obtained for these cases using only 20,000 MCS passes, but all other settings remained the same. The measured and predicted energy spectra for reactor power levels of 300 kW, 500 kW, and 800 kW are shown together in Figure 5. These results indicate that the reactor power level does not significantly affect the shape of the neutron spectrum. Also, the deviation due to Bi crystalline effects is still observed at lower power levels, with consistent position and relative prominence.

In spite of this deviation, the experimentally-measured data show remarkable agreement with the modeled spectra. For neutron speeds less than 5000 m/s and energies less than 0.1 eV, the average fractional deviation between measured and modeled values is 7.1%. Over the entire spectrum, the average fractional deviation is 18.5%.

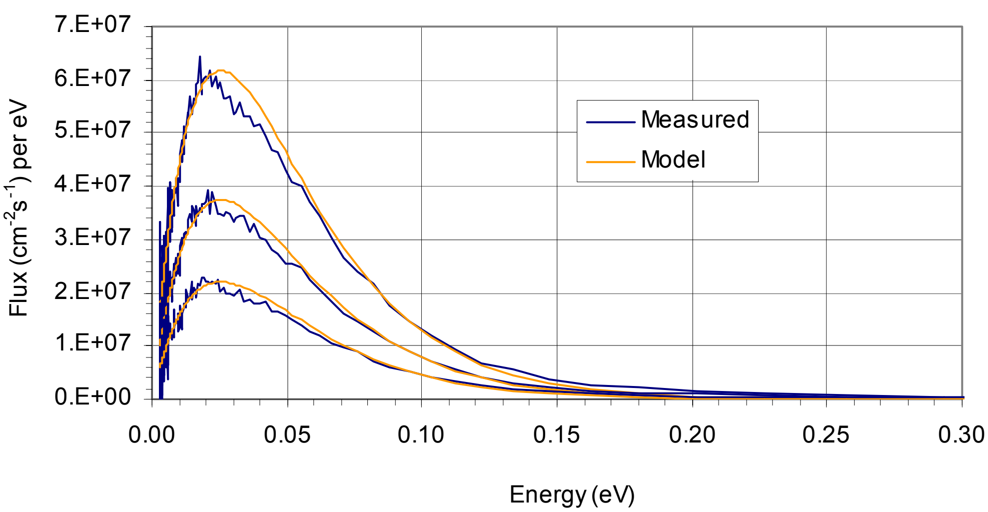

Fig. 5. Neutron energy spectrum measured at 300 kWt, 500 kWt, and 800 kWt.

9. Conclusions and future work

These results show that the chopper spectrometer and TOF method yield an accurate result. Spectra obtained using this simple instrument match the Maxwellian-based models to within less than 20%, and reconfirm the distinctive thermal shape expected for the RSEC primary neutron beam. The simplicity of this design introduces high levels of uncertainty in measured data, and some discrepancies are apparent. But the data processing technique described here allows the most dominant effects of the experimental environment to be accounted for, resulting in a clear measurement of the neutron spectrum. The valuable information contained in this data easily justifies the minimal effort and funding required to make the chopper system operational. It is anticipated that future refinements of this developmental model will yield a more accurate and robust instrument and, possibly, a spectrometer for thermal neutron beams that is both accurate and portable.

References

1) J. Niederhaus, M.S. thesis, Pennsylvania State University, University Park, PA (2003).
2) J. Niederhaus, J. Brenizer, and K. Ünlü, "Thermal Neutron Time-of-Flight Spectroscopy at Penn State using a Single-Disk Chopper," *Trans. Am. Nuc. Soc.*, **89**, 677 (2003).
3) T. Emoto, Ph.D. thesis, Cornell University, Ithaca, NY (1990).
4) S. Spern, Ph.D. thesis, Cornell University, Ithaca, NY (1998).
5) A. Foster and R. Wright, *Basic Nuclear Engineering*, Fourth Edition, Pearson Allyn & Bacon, Inc., 1983.
6) E. B. Iverson, ORNL/SNS, personal communication.